HHS Public Access

Author manuscript

Biol Psychiatry Cogn Neurosci Neuroimaging. Author manuscript; available in PMC 2020 February 01.

Published in final edited form as:

Biol Psychiatry Cogn Neurosci Neuroimaging. 2019 February ; 4(2): 171–179. doi:10.1016/j.bpsc.2018.07.013.

Abnormal prefrontal development in pediatric posttraumatic stress disorder: a longitudinal structural and functional magnetic resonance imaging study

Sara A. Heyn, MS, JD[1,2], **Taylor J. Keding, BS**[2], **Marisa C. Ross, BS**[2], **Josh M. Cisler, PhD**[2,3], **Jeanette A. Mumford, PhD**[4], and **Ryan J. Herringa, MD, PhD**[2,3]

[1]Neuroscience & Public Policy Program, University of Wisconsin-Madison, Madison, WI, USA

[2]Neuroscience Training Program, University of Wisconsin-Madison, Madison, WI, USA

[3]Department of Psychiatry, University of Wisconsin-Madison School of Medicine and Public Health, Madison, WI, USA

[4]Center for Healthy Minds, University of Wisconsin-Madison, Madison, WI, USA

Abstract

Background: Prior studies of pediatric posttraumatic stress disorder (PTSD) have reported cross-sectional and age-related structural and functional brain abnormalities in networks associated with cognitive, affective, and self-referential processing. However, no reported studies have comprehensively examined longitudinal gray matter development and its intrinsic functional correlates in pediatric PTSD.

Methods: Twenty-seven youth with PTSD and twenty-one non-traumatized typically developing (TD) youth were assessed at baseline and one-year follow-up. At each visit, youth completed structural MRI and resting-state functional MRI. Regions with volumetric abnormalities in the whole-brain structural analyses were identified and used as seeds in exploratory intrinsic connectivity analyses.

Results: Youth with PTSD exhibited sustained reductions in grey matter volume (GMV) in right ventromedial prefrontal cortex (vmPFC) and bilateral ventrolateral prefrontal cortex (vlPFC). Group by time analyses revealed aberrant longitudinal development in dorsolateral prefrontal cortex (dlPFC) where TD youth exhibited normative decreases in GMV between baseline and follow-up while youth with PTSD showed increases in GMV. Using these regions as seeds, PTSD patients exhibited atypical longitudinal decreases in intrinsic prefrontal-amygdala and -hippocampus connectivity, in contrast to increases in TD youth. Specifically, youth with PTSD showed decreasing vmPFC-amygdala connectivity as well as decreasing vlPFC-hippocampus connectivity over time. Notably, volumetric abnormalities in the vmPFC and vlPFC were predictive of symptom severity.

Corresponding Author: Sara Heyn, University of Wisconsin-Madison, Department of Psychiatry, BRAVE Youth Lab, 6001 Research Park Blvd. Rm 1329, Madison, WI 53719, sheyn@wisc.edu.

DISCLOSURES

The authors report no biomedical financial interests or potential conflicts of interest.

This data was previously presented at the Society for Research in Child Development Biennial Meeting (Austin, TX; April 6–8, 2017).

Conclusions: These findings represent novel longitudinal volumetric and connectivity changes in pediatric PTSD. Atypical prefrontal GMV and prefrontal-amygdala and-hippocampus development may underlie persistence of PTSD in youth and could serve as future therapeutic targets.

Keywords

Posttraumatic stress disorder; structural magnetic resonance imaging; functional magnetic resonance imaging; pediatric; Neurodevelopment; Childhood Trauma

INTRODUCTION

Pediatric posttraumatic stress disorder (PTSD) is classically characterized by reexperiencing, avoidance, and hyperarousal symptoms associated with childhood trauma exposure, as well as changes in negative affect and cognition (1). PTSD is common in youth, with a lifetime prevalence of 4.7% and a point prevalence of 1.6% (2). Recent neuroimaging studies of pediatric PTSD suggest a pattern of neural abnormalities that are not simply a recapitulation of adult PTSD, but rather interact with dynamic structural and functional brain changes occurring in development. However, little is known about neural mechanisms underlying the maintenance of and recovery from PTSD over the course of development. Neurodevelopmental abnormalities in gray matter volume (GMV) and resting state functional connectivity (RSFC) together may help to illuminate the pathway of PTSD progression across childhood. However, to date, no reported studies have longitudinally investigated pediatric PTSD across these domains.

Cross-sectional studies of pediatric PTSD point to abnormal structure and function in prefrontal-amygdala and -hippocampus circuitry implicated in cognitive-emotional control and threat extinction (3). Two recent studies, including our own, showed that youth with PTSD have decreased GMV in the ventromedial prefrontal cortex (vmPFC) relative to non-traumatized typically developing (TD) (4) and trauma-exposed comparison (TEC) youth (5). Structural abnormalities in the amygdala and hippocampus have been more variable. Using both region of interest and voxelwise approaches, youth with PTSD show no differences in amygdala or hippocampal GMV relative to TD youth (4–7). However, TEC youth appear to have increased amygdala and hippocampal GMV relative to PTSD and TD youth, suggesting possible correlates of trauma resilience. Given reports of reduced hippocampal GMV in adult PTSD (8), the lack of deficits in pediatric PTSD may represent a delayed developmental effect in the hippocampus. Consistent with this notion, we found that youth with PTSD show decreased hippocampal volume with (cross-sectional) age, in contrast to increased volume with age in TD youth (4). Together, these findings suggest that reduced vmPFC volume and disrupted hippocampal development in youth with PTSD may contribute to deficits in cognitive-emotional control and threat extinction as youth age. To date, only pilot studies have longitudinally examined structural brain development in pediatric PTSD relative to comparison youth using ROI-based approaches (9,10). Larger studies of whole-brain morphometry are important to determine whether structural abnormalities persist, and whether additional prefrontal changes may contribute to symptom persistence or recovery.

Functional MRI studies of pediatric PTSD also suggest abnormal communication between medial prefrontal regions and the amygdala and hippocampus which may underlie illness expression. In emotion processing tasks, we have shown that youth with PTSD demonstrate decreased amygdala-mPFC coupling to aversive stimuli (11–13), as well as decreased amygdala-vmPFC coupling with age (11). To date, only one reported study examined intrinsic prefrontal coupling with the amygdala/hippocampus in pediatric PTSD, though did not examine age-related effects. Youth with PTSD showed decreased coupling between the basolateral amygdala and mPFC, but increased centromedial amygdala-orbitofrontal cortex coupling relative to TD youth (14). Overall, these studies suggest impaired amygdala-mPFC coupling in pediatric PTSD, which may further contribute to deficits in cognitive-emotional control as youth age. However, it remains unclear how structural brain abnormalities relate to intrinsic communication, nor whether longitudinal changes in these circuits may contribute to symptom development in afflicted youth.

Here, we provide the first whole-brain, longitudinal assessment of neurodevelopment in youth with PTSD using multimodal imaging. We first investigated structural morphometry, with the prediction that youth with PTSD would have persistent reductions in vmPFC volume and declining hippocampal volume over time. In exploratory analyses, we then seeded prefrontal regions that exhibited sustained or longitudinal GMV changes to investigate how structural abnormalities relate to resting-state functional connectivity with the amygdala-hippocampus complex. Based upon our previous work, we hypothesized declining medial prefrontal-amygdala and hippocampus connectivity over time, which in turn would correlate with symptom severity.

METHODS AND MATERIALS

Participants

Participants included 36 medication-free (at baseline) youth with PTSD and 21 non-traumatized typically developing (TD) youth between the ages of 8 to 18 recruited from local mental health facilities and the general community, respectively. Exclusion criteria for youth with PTSD at study entry included IQ<70; history of psychotic disorder, bipolar disorder, or OCD; active suicidality; recent (past 4 weeks) substance abuse or dependence; unstable medical condition; recent use of psychotropic medication (past 4 weeks, 6 weeks for fluoxetine); MRI contraindication; and pregnancy in females. No participants were taken off any psychotropic medication for the purposes of this study. Parental consent and youth assent were obtained for all participants and all procedures used were approved by the University of Wisconsin Health Sciences IRB. The majority of both groups were retained for both a baseline and follow-up visit, leaving 27 youth with PTSD and 21 TD youth in the final analyses.

All youth were assessed with structured trauma and psychiatric interviews with the Kiddie Schedule for Affective Disorders and Schizophrenia (KSADS; (15)) at both time points. A PTSD diagnosis was determined using modified DSM-IV criteria (16) through a combination of the KSADS and the Clinician-Administered PTSD Scale for Children and Adolescents (CAPS-CA; (17)). IQ scores for all youth were estimated using the Full-Scale IQ-2 component of the Wechsler Abbreviated Scale of Intelligence-II (18). One of the PTSD

youth was not able complete the full baseline IQ testing due to fatigue. All youth completed the following additional assessments: the Mood and Feelings Questionnaire (MFQ; (19)), the Screen for Child Anxiety Related Emotional Disorders (SCARED; (20)), and the Stressful Life Events Schedule Adolescent Self-Report (SLES; (21)). PTSD youth also completed the UCLA PTSD Reaction Index (PTSD-RI; (22)). Further details regarding participant recruitment and assessment have been previously described (4,11,13).

VOXEL-BASED MORPHOMETRY

sMRI Acquisition and Preprocessing

Prior to both the baseline and follow-up scan, youth completed two mock scanning sessions in order to accommodate them to the scanning environment and optimize data yield. Magnetic resonance images were acquired using a 3.0T GE Discovery MR750 scanner with an 8-channel radiofrequency head coil (General Electric, Milwaukee, WI) at the University of Wisconsin Department of Psychiatry. Three-dimensional axial high-resolution T1 images were acquired with the following parameters: echo time = 3.18 ms, repetition time = 8.16 ms, inversion time = 450 ms, flip angle = 12°, field of view = 25.6 cm, slice thickness: 1.0 mm, 156 slices, and image matrix 256 × 256 that covered the entire brain. For whole-brain voxel-based morphometry (VBM) preprocessing was performed using the Computational Anatomy (CAT12) toolbox (http://dbm.neuro.uni-jena.de/cat/) in SPM12 (Wellcome Department of Imaging Neuroscience, London, UK) in Matlab 8.3. The T1-weighted images were first processed using longitudinal segmentation, a rigid within-subject realignment, and one spatial normalization to all time points using default parameters in CAT12. Modulation and normalization of images included both affine and non-linear registration. After preprocessing of structural images, the covariance structure of all gray matter images was checked for homogeneity with all other images. Final voxel resolution was 1.5 × 1.5 × 1.5 mm.

Of the total sample, 22 PTSD and 20 TD youth were included in final VBM analyses. One PTSD participant was excluded due to covariance being more than two SD below the mean, due to significant motion artifact on close inspection. Three additional participants were not included (2 PTSD and 1 TD), because the follow-up visit occurred after VBM analysis.

Statistical Analyses

Analyses on demographic and clinical data were examined using a 2-tailed unpaired *t* test, while categorical data were assessed using χ^2 tests. R version 3.3.0 (23) and RStudio (24) were used for these analyses. For the longitudinal gray matter volume (GMV) analysis (PTSD vs. TD), a general linear-mixed effects model was used to compute a voxel-wise map of the main effect of group and a group by time interaction term, adjusting for age at baseline, sex, total intracranial volume (TIV), and subject as a random effect. Model parameters were estimated using AFNI's 3dLME (25). Whole brain family-wise error correction was performed using Monte Carlo simulation (AFNI's 3dClustSim, -acf option). At an individual voxel threshold of $p = 0.005$, the whole-brain cluster threshold was 495 voxels, resulting in $p_{FWE} < 0.05$.

RESTING-STATE FUNCTIONAL CONNECTIVITY

fMRI Acquisition and Preprocessing

Resting state functional data was collected at the same slice locations as the T1-weighted anatomical data. The resting-state fMRI was obtained using an echo-planar imaging (EPI) pulse sequence with the following parameters: sagittal orientation, TE=22 milliseconds, TR = 2150 milliseconds, flip angle = 79 degrees, slice thickness = 3mm, gap = 0.5mm, 41 slices, FOV = 224mm, and matrix size = 64 × 64. The scan lasted 5 minutes and 16 seconds (TR = 146). During this time, youth were instructed to stay awake and rest with their eyes open, but not to think of anything in particular. All preprocessing, including longitudinal registration, of individual resting-state scans at both time points was carried out in AFNI (26). Preprocessing of individual scans included: (1) deletion of the first 3 volumes, (2) statistical outlier detection and despiking of fMRI data, (3) slice-timing correction, (4) co-registration of T1 and EPI images and realignment of EPI volumes, (5) motion correction and spatial smoothing (6 mm full width at half maximum [FWHM]), anatomy segmentation, (6) and nuisance regression (eroded white matter, cerebrospinal fluid, 6 motion parameters and their derivatives) and motion censoring in a single step. Volumes were motion censored using a threshold of 0.25 mm based on frame-wise displacement calculated using the Euclidean norm.

During longitudinal registration, the T1 anatomical images at each time point were aligned and a transformation matrix was output. The inverse, square-root-transformed mean transformation matrix was calculated and applied to each of the T1 images. The mean of the resulting images was calculated and then normalized to the Montreal Neurological Institute (MNI) template. The square-root-transformed mean transformation matrix was then applied to the raw EPI datasets, the residual datasets from the aforementioned nuisance regression (output of *3dREMLfit*), and the whole-brain masks at each time point. An intersection mask combining each time point's aligned mask was applied to each residual dataset, resulting in an output with only voxels in common between the two time points. Following longitudinal registration, temporal filtering (0.01 Hz<f<0.1Hz) was applied to the time series of each voxel. Participants having 25% of volumes flagged by the motion censoring algorithm (in either the time one or time two images) were excluded from the study. The average motion in all directions was calculated and compared across groups, with no differences in motion observed. Final voxel resolution was 2 × 2 × 2 mm.

Of the total sample, 22 PTSD youth and 21 TD controls were included in the final RSFC analyses. Seven youth were excluded due to motion artifact (PTSD, n=3) or to follow-up scans that occurred after the VBM analyses had been completed (PTSD, n=3; TD, n=1).

Statistical Analyses

An exploratory seed-based connectivity analysis was then conducted using prefrontal regions identified in the VBM analyses: left and right vlPFC, vmPFC, and left dlPFC (resampled to EPI grid space). Pearson product-moment correlation coefficients were calculated between the average time course of each seed and all other voxels in the brain, converted to z values using the Fisher-Z transform, and entered into a second-level random-

effects analysis implemented in AFNI. We used a linear mixed-effects model incorporating random effects in order to assess connectivity estimates as a function of group and group by time, adjusting for age at baseline, sex, and subject as a random effect. We conducted analyses in the *a priori* search region of the amygdala/hippocampus, which was created in AFNI by combining the bilateral amygdala and hippocampus ROIs (derived from (27)) included in the Anatomical Automatic Labeling (AAL) atlas (http://neuro.imm.dtu.dk/wiki/Automated_Anatomical_Labeling). While these subcortical analyses were performed in order to explore the structural abnormalities identified in the primary VBM analyses, whole-brain analyses have been included in the Supplement. Whole brain family-wise error correction across all five seed-based analyses was performed using Monte Carlo simulation (AFNI's 3dClustSim, -acf option). At an individual voxel threshold of $p = 0.005$, the cluster threshold was 20 voxels for the amygdala-hippocampus mask and 699 voxels for the whole-brain analyses, resulting in $p_{FWE} < 0.05$. Given the exploratory nature of the RSFC analyses, we did not apply additional multiple comparison correction across the separate seed-based analyses.

RESULTS

Participant Characteristics

Participant characteristics are shown in Tables 1 and 2. Across groups, the average interscan interval was 1.22 years (See Supplemental Figure 1). There were no differences between groups for sex, age, Tanner stage, or length of time between scans (p>0.05). There was a significant group difference in IQ, with modestly lower IQ in the PTSD group (t=2.53, df=44, p=0.015, Table 1). On average, PTSD symptom severity (as measured by the PTSD-RI score) decreased by 32% between the baseline and follow-up scan (t=3.33, df=24, p=0.003; Table 2). Of the 27 PTSD youth, 11 had taken psychiatric medication before baseline and 11 took psychiatric medication between baseline and follow-up. At the follow-up scan, 14 of the 27 PTSD youth still met criteria for a PTSD diagnosis. Finally, almost all PTSD youth were diagnosed with a comorbid disorder at either baseline (n=21) or follow-up (n=17).

Longitudinal Voxel-based Morphometry: Whole Brain Analyses

Whole-brain VBM results are summarized in Table 3. In both groups, decreases in GMV were found across the entire cortex over time (Figure 2). Group main effects revealed sustained decreases in GMV in the right anterior vmPFC (BA 10/11), bilateral vlPFC (BA 45/47), right precentral gyrus (BA 44), and PCC (BA 31) in youth with PTSD (Figure 1). A significant group by time effect was observed in the left dlPFC (BA 9). Here, GMV in the dlPFC decreased over time in TD youth, while youth with PTSD showed slightly increasing GMV over time (Figure 1). Separate multivariate regressions within the PTSD youth on the group main effects and six symptom domains (MFQ, SCARED, PTSD-RI subscore B/C/D, and PTSD-RI total; covaried for age at baseline, sex, and TIV) revealed three significant symptom relationships. GMV in the left vlPFC is negatively predictive of depression symptoms (MFQ; df=38, t=−2.24, p=0.03; Figure 1), GMV in the vmPFC was negatively predictive of re-experiencing symptoms (PTSD-RI subscore B; df=38, t=−2.01, p=0.05;

Figure 1), and PCC GMV was positively predictive of overall PTSD symptom severity (PTSD-RI total; df=38, t=2.192, p=0.02).

Resting-State Prefrontal Connectivity: Seed-Based Analyses

Among the sustained and developmental abnormalities identified in the VBM analyses, we were interested in interrogating the four prefrontal regions identified: bilateral vlPFC, vmPFC, and dlPFC. Here we report RSFC findings within our *a priori* amygdala-hippocampal search region, summarized in Table 4. In a significant group x time interaction, youth with PTSD exhibited aberrant longitudinal intrinsic functional connectivity between the vmPFC and left amygdala ([26,8,−16]; k=26; Z=−3.79). Specifically, TD youth showed increasing (more positive) connectivity over time while youth with PTSD showed decreasing (more negative) connectivity over time (Figure 3). An additional significant group x time interaction revealed abnormal intrinsic connectivity between the left vlPFC and the left anterior hippocampus ([32,12,−18]; k=22; Z=−3.95). The dlPFC seed also showed a group by time interaction with the left anterior hippocampus at trend level ([34, 18,−24]; k=17; Z=−3.22; p=0.07). In both cases, TD youth showed increasing (more positive) connectivity over time while youth with PTSD exhibited the opposite effect (Figure 3). Separate multivariate regressions within the PTSD youth on connectivity findings revealed symptom relationships only with dlPFC-hippocampus connectivity. Here, dlPFC-hippocampus coupling was inversely related to anxiety, depression, and PTSD severity (see Supplemental Material).

Post hoc Analyses

All remaining post hoc analyses are fully described in the Supplement but are briefly reviewed here. Across all morphometric and functional connectivity analyses, all group and group by time findings remained statistically significant or near significant when adjusting for other potential explanatory variable measures, including IQ, Tanner stage, trauma load, age at index trauma, previous use of any type of psychiatric medication, or history of psychotherapy. It is important to note that while the exploratory analyses above suggest that lack of significant abnormalities in hippocampal GMV was driven by interim SSRI use, post hoc analyses on regions with significant structural abnormalities were not significantly influenced by psychiatric medication use. Finally, the perceived impact of stressful life events before baseline and between time points was not predictive of any of the structural or functional abnormalities identified.

DISCUSSION

To our knowledge, this is the first multimodal, longitudinal analysis of neurodevelopment in pediatric PTSD. We report novel findings including sustained reductions and abnormal neurodevelopment in key prefrontal nodes in youth with PTSD as compared to typically developing youth. Specifically, we have replicated reduced vmPFC gray matter volume found in our previous cross-sectional analysis of the baseline cohort in this longitudinal analysis (4), as well as identifying additional regions in the vlPFC showing sustained GMV reductions. Further, youth with PTSD exhibit abnormal increases in dlPFC volume in contrast to normative, widespread decreases elsewhere in the cortex. Notably, these

prefrontal nodes with structural abnormalities also showed evidence of declining intrinsic connectivity with the amygdala/hippocampus complex over time in youth with PTSD in subsequent exploratory analyses. These results suggest that prefrontal structural abnormalities may reflect abnormal development of intrinsic prefrontal network function in youth with PTSD.

Our findings are highly consistent with existing circuit models of PTSD and psychopathology more broadly. Reduced vmPFC volume has now been demonstrated in both adult and pediatric PTSD, and the present findings suggest that this reflects a sustained pattern in pediatric PTSD. The vmPFC is notable for its role in the top-down modulation of amygdala responses and the inhibition of threat responses in both humans and rats (30,31). Consistent with this notion, we also observed reductions in vmPFC-amygdala connectivity over time in youth with PTSD. This stands in contrast to increased coupling over time in our TD youth, as well as documented cross-sectional age-related increases in vmPFC-amygdala intrinsic connectivity in TD youth (32). Furthermore, these findings are consistent with reduced basolateral amygdala (BLA)-mPFC intrinsic connectivity previously reported in adolescent PTSD (14). Taken together, these findings suggest that vmPFC structural abnormalities and reduced vmPFCamygdala coupling over time may contribute to threat extinction deficits in pediatric PTSD which may worsen with age.

Next, we also found evidence of volumetric abnormalities in the vlPFC and dlPFC, which represent novel findings in pediatric PTSD. Here, youth with PTSD exhibited sustained reductions in GMV in bilateral vlPFC as well as abnormal increases in GMV in the dlPFC. The vlPFC and dlPFC have both been heavily implicated in emotion regulation processes (33,34). In particular, the vlPFC is involved in selection and inhibition of cognitive appraisals (33,35), while the dlPFC has consistently been associated with the explicit emotion regulation through cognitive reappraisal (33,36,37). Interestingly, both of these nodes showed evidence of reduced intrinsic connectivity over time with the anterior hippocampus, in contrast to increases in TD youth. The hippocampus is known to be involved in the contextual regulation of emotion including gating of conditioned threat responses. However, the anterior hippocampus, which has extensive amygdala projections, is also preferentially involved in unconditioned threat responses. While neither VBM nor RSFC analyses are inherently able to provide information regarding the functional significance of regions identified as having group or longitudinal abnormalities, we speculate based upon the prior literature that our observed decreases in vlPFC/dlPFC-hippocampus connectivity in youth with PTSD may reflect loss of inhibitory control of unconditioned threat responses over time and could conceivably contribute to increasing threat acquisition and impaired threat extinction in pediatric PTSD. This notion is further supported by the symptom relationships identified between dlPFC-hippocampus connectivity and anxiety, depression, and PTSD symptom severity (Supplemental Figure 2). However, future studies specifically incorporating threat learning and emotion regulation tasks will clearly be needed to address these possibilities.

Surprisingly, we were unable to detect abnormal volumetric change in the hippocampus over a one-year period in the youth with PTSD. Our prior study, albeit cross-sectional, found evidence of decreased right anterior hippocampal volume with age in youth with PTSD (2).

Even with signal averaging across voxels over a hippocampal ROI, we were unable to detect an association between hippocampal volume and PTSD. Based on the ROI data, the estimated chance of Type II error is beta=.28. One possible explanation could be that medication exposure in youth with PTSD is masking these effects. Notably, SSRIs are known to increase hippocampal neurogenesis (28,29), and appear to increase hippocampal gray matter volume in adults with PTSD (38,39). Intriguingly, an exploratory analysis revealed an interaction effect with SSRI use in the right anterior hippocampus. Youth with PTSD that had taken SSRI between baseline and follow-up (n=6) showed increased hippocampal GMV over time compared to non-SSRI exposed youth with PTSD (n=16) or TD youth (n=20) (See Supplemental Figure 2). While preliminary, these findings suggest that SSRI use may counteract hippocampal volume decline in youth with PTSD. Further study in larger samples of youth in a randomized controlled treatment design would be warranted to determine whether SSRI use is indeed capable of augmenting hippocampal volume in youth with PTSD. Similarly, future studies would be warranted to determine whether current evidence-based therapies such as TF-CBT are capable of "correcting" prefrontal volumetric deficits in pediatric PTSD, and to what extent gray matter volume and RSFC changes may mediate the effects of treatment. Notably, recent studies in adult PTSD (40–42) suggest that both psychotherapy and SSRI treatment may augment function in prefrontal regions (vlPFC, dlPFC) implicated in cognitive-emotional control.

Although this study has identified novel neurodevelopmental abnormalities in prefrontal-amygdala and hippocampus circuitry in pediatric PTSD, it is not without limitations. First, although we strove to appropriately match our groups and adjust for potentially confounding variables in post hoc analyses, we cannot rule out the possibility that these results could be accounted for by an unknown third variable. Second, youth were allowed to receive treatment as usual in the community. However, all were unmedicated at the time of the baseline scan and all results remained significant after adjusting for medication and psychotherapy. Third, our sample is only moderate in size with a single follow-up scan. A replication and/or extension of our current study to multiple time points with a larger sample size is warranted. Finally, our cohort of youth with PTSD recruited were typically exposed to more than one trauma. Age and chronicity of trauma exposure are likely influential factors on prefrontal-amygdala and -hippocampal development as well as other circuits (43). However, given our moderate sample size, we were not able to fully explore sensitive periods with regard to the neural abnormalities identified. Finally, in order to differentiate the effects specific to PTSD from the general effects of childhood trauma, future studies should include a trauma-exposed group.

In summary, our results provide the first longitudinal evidence of sustained and developmental structural and functional abnormalities in key prefrontal-amygdala and hippocampus circuits in pediatric PTSD. Notably, reduced volume and abnormal development in these prefrontal nodes was associated with declining functional connectivity over time with the amygdala-hippocampus complex, implicating these prefrontal circuits in the persistence of PTSD and its comorbidities in developing youth. Future studies would be merited to further explore the diagnostic specificity of these developmental patterns, and test whether current evidence-based treatments are capable of "restoring" healthy neurodevelopment, or compensatory neurodevelopment, in youth suffering from PTSD.

Supplementary Material

Refer to Web version on PubMed Central for supplementary material.

ACKNOWLEDGEMENTS

We would like to especially thank Rachael Meline and Shelby Weaver for their work in the recruitment and data collection for this study.

Funding for this study was provided by the National Institute of Mental Health Career Development Award (K08 MH100267, to RJH), American Academy of Child and Adolescent Psychiatry Junior Investigator Award (to RJH), NARSAD Young Investigator Grant (to RJH), University of Wisconsin Institute for Clinical and Translational Research Translational Pilot Grant Award (NIH/NCATS UL1TR000427, to RJH), University of Wisconsin Institute of Clinical and Translational TL1 Training Award (TL1TR000429, to SAH), and the University of Wisconsin School of Medicine and Public Health. None of these funding sources had a direct effect in the design, analysis, or interpretation of the study results, nor in preparation of the manuscript.

This material is based upon work supported by the National Science Foundation Graduate Research Fellowship Program under Grant No. DGE-1747503 (to TJK). Any opinions, findings, and conclusions or recommendations expressed in this material are those of the author(s) and do not necessarily reflect the views of the National Science Foundation. Support was also provided by the Graduate School and the Office of the Vice Chancellor for Research and Graduate Education at the University of Wisconsin-Madison with funding from the Wisconsin Alumni Research Foundation.

REFERENCES

1. American Psychiatric Association Diagnostic and statistical manual of mental disorders: DSM-5. 5th ed. Washington, D.C: American Psychiatric Association; 2013.
2. McLaughlin KA, Koenen KC, Hill ED, Petukhova M, Sampson NA, Zaslavsky AM, et al. Trauma exposure and posttraumatic stress disorder in a national sample of adolescents. J Am Acad Child Adolesc Psychiatry. 2013 8;52(8):815–830.e14. [PubMed: 23880492]
3. Herringa RJ. Trauma, PTSD, and the Developing Brain. Curr Psychiatry Rep. 2017 10 1;19(10):69. [PubMed: 28823091]
4. Keding TJ, Herringa RJ. Abnormal structure of fear circuitry in pediatric post-traumatic stress disorder. Neuropsychopharmacol Off Publ Am Coll Neuropsychopharmacol. 2015 2;40(3):537–45.
5. Morey RA, Haswell CC, Hooper SR, De Bellis MD. Amygdala, Hippocampus, and Ventral Medial Prefrontal Cortex Volumes Differ in Maltreated Youth with and without Chronic Posttraumatic Stress Disorder. Neuropsychopharmacology. 2016 2;41(3):791–801. [PubMed: 26171720]
6. Carrion VG, Weems CF, Eliez S, Patwardhan A, Brown W, Ray RD, et al. Attenuation of frontal asymmetry in pediatric posttraumatic stress disorder. Biol Psychiatry. 2001 12 15;50(12):943–51. [PubMed: 11750890]
7. De Bellis MD, Keshavan MS, Shifflett H, Iyengar S, Beers SR, Hall J, et al. Brain structures in pediatric maltreatment-related posttraumatic stress disorder: a sociodemographically matched study. Biol Psychiatry. 2002 12 1;52(11):1066–78. [PubMed: 12460690]
8. Kuhn S, Gallinat J. Gray matter correlates of posttraumatic stress disorder: a quantitative meta-analysis. Biol Psychiatry. 2013 1 1;73(1):70–4. [PubMed: 22840760]
9. De Bellis MD, Hall J, Boring AM, Frustaci K, Moritz G. A pilot longitudinal study of hippocampal volumes in pediatric maltreatment-related posttraumatic stress disorder. Biol Psychiatry. 2001 8 15;50(4):305–9. [PubMed: 11522266]
10. Carrion VG, Weems CF, Reiss AL. Stress predicts brain changes in children: a pilot longitudinal study on youth stress, posttraumatic stress disorder, and the hippocampus. Pediatrics. 2007 3;119(3):509–16. [PubMed: 17332204]
11. Wolf RC, Herringa RJ. Prefrontal-Amygdala Dysregulation to Threat in Pediatric Posttraumatic Stress Disorder. Neuropsychopharmacol Off Publ Am Coll Neuropsychopharmacol. 2016 2;41(3): 822–31.

12. Cisler JM, Scott Steele J, Smitherman S, Lenow JK, Kilts CD. Neural processing correlates of assaultive violence exposure and PTSD symptoms during implicit threat processing: A network-level analysis among adolescent girls. Psychiatry Res. 2013 12 30;214(3):238–46. [PubMed: 23969000]
13. Keding TJ, Herringa RJ. Paradoxical Prefrontal-Amygdala Recruitment to Angry and Happy Expressions in Pediatric Posttraumatic Stress Disorder. Neuropsychopharmacol Off Publ Am Coll Neuropsychopharmacol. 2016 Nov;41(12):2903–12.
14. Aghajani M, Veer IM, van Hoof M-J, Rombouts SARB, van der Wee NJ, Vermeiren RRJM. Abnormal functional architecture of amygdala-centered networks in adolescent posttraumatic stress disorder. Hum Brain Mapp. 2016 3;37(3):1120–35. [PubMed: 26859310]
15. Kaufman J, Birmaher B, Brent D, Rao U, Flynn C, Moreci P, et al. Schedule for Affective Disorders and Schizophrenia for School-Age Children-Present and Lifetime Version (KSADS-PL): initial reliability and validity data. J Am Acad Child Adolesc Psychiatry. 1997 7;36(7):980–8. [PubMed: 9204677]
16. Cohen JA, Mannarino AP, Iyengar S. Community treatment of posttraumatic stress disorder for children exposed to intimate partner violence: a randomized controlled trial. Arch Pediatr Adolesc Med. 2011 1;165(1):16–21. [PubMed: 21199975]
17. Weathers FW, Keane TM, Davidson JR. Clinician-administered PTSD scale: a review of the first ten years of research. Depress Anxiety. 2001;13(3):132–56. [PubMed: 11387733]
18. Wechsler D Wechsler Abbreviated Scale of Intelligence–Second Edition Manual. Bloomington, MN: Pearson; 2011.
19. Costello EJ, Angold A. Scales to assess child and adolescent depression: checklists, screens, and nets. J Am Acad Child Adolesc Psychiatry. 1988 11;27(6):726–37. [PubMed: 3058677]
20. Birmaher B, Khetarpal S, Brent D, Cully M, Balach L, Kaufman J, et al. The Screen for Child Anxiety Related Emotional Disorders (SCARED): scale construction and psychometric characteristics. J Am Acad Child Adolesc Psychiatry. 1997 4;36(4):545–53. [PubMed: 9100430]
21. Williamson DE, Birmaher B, Ryan ND, Shiffrin TP, Lusky JA, Protopapa J, et al. The stressful life events schedule for children and adolescents: development and validation. Psychiatry Res. 2003 8 1;119(3):225–41. [PubMed: 12914894]
22. Steinberg AM, Brymer MJ, Decker KB, Pynoos RS. The University of California at Los Angeles Post-traumatic Stress Disorder Reaction Index. Curr Psychiatry Rep. 2004 4;6(2):96–100. [PubMed: 15038911]
23. R Core Team. R: A Language and Environment for Statistical Computing [Internet]. Vienna, Austria: R Foundation for Statistical Computing; 2013 Available from: https://www.R-project.org
24. RSTudio Team. RStudio: Integrated Development for R. Boston, MA: RStudio, Inc.; 2012.
25. Chen G, Saad ZS, Britton JC, Pine DS, Cox RW. Linear mixed-effects modeling approach to FMRI group analysis. NeuroImage. 2013 6 1;73:176–90. [PubMed: 23376789]
26. Cox RW. AFNI: software for analysis and visualization of functional magnetic resonance neuroimages. Comput Biomed Res Int J. 1996 6;29(3):162–73.
27. Amunts K, Kedo O, Kindler M, Pieperhoff P, Mohlberg H, Shah NJ, et al. Cytoarchitectonic mapping of the human amygdala, hippocampal region and entorhinal cortex: intersubject variability and probability maps. Anat Embryol (Berl). 2005 12;210(5–6):343–52. [PubMed: 16208455]
28. Santarelli L, Saxe M, Gross C, Surget A, Battaglia F, Dulawa S, et al. Requirement of hippocampal neurogenesis for the behavioral effects of antidepressants. Science. 2003 8 8;301(5634):805–9. [PubMed: 12907793]
29. Powell TR, Murphy T, de Jong S, Lee SH, Tansey KE, Hodgson K, et al. The genome-wide expression effects of escitalopram and its relationship to neurogenesis, hippocampal volume, and antidepressant response. Am J Med Genet Part B Neuropsychiatr Genet Off Publ Int Soc Psychiatr Genet. 2017 6;174(4):427–34.
30. Milad MR, Quirk GJ. Neurons in medial prefrontal cortex signal memory for fear extinction. Nature. 2002 11 7;420(6911):70–4. [PubMed: 12422216]

31. Rougemont-Bücking A, Linnman C, Zeffiro TA, Zeidan MA, Lebron-Milad K, RodriguezRomaguera J, et al. Altered processing of contextual information during fear extinction in PTSD: an fMRI study. CNS Neurosci Ther. 2011 8;17(4):227–36. [PubMed: 20406268]
32. Gabard-Durnam LJ, Flannery J, Goff B, Gee DG, Humphreys KL, Telzer E, et al. The development of human amygdala functional connectivity at rest from 4 to 23 years: a crosssectional study. NeuroImage. 2014 7 15;95:193–207. [PubMed: 24662579]
33. Buhle JT, Silvers JA, Wager TD, Lopez R, Onyemekwu C, Kober H, et al. Cognitive Reappraisal of Emotion: A Meta-Analysis of Human Neuroimaging Studies. Cereb Cortex. 2014 11 1;24(11): 2981–90. [PubMed: 23765157]
34. Wager TD, Davidson ML, Hughes BL, Lindquist MA, Ochsner KN. Prefrontal-Subcortical Pathways Mediating Successful Emotion Regulation. Neuron. 2008 9 25;59(6):1037–50. [PubMed: 18817740]
35. Robbins TW. Shifting and stopping: fronto-striatal substrates, neurochemical modulation and clinical implications. Philos Trans R Soc Lond B Biol Sci. 2007 5 29;362(1481):917–32. [PubMed: 17412678]
36. Goldin PR, McRae K, Ramel W, Gross JJ. The Neural Bases of Emotion Regulation: Reappraisal and Suppression of Negative Emotion. Biol Psychiatry. 2008 3 15;63(6):577–86. [PubMed: 17888411]
37. McRae K, Gross JJ, Weber J, Robertson ER, Sokol-Hessner P, Ray RD, et al. The development of emotion regulation: an fMRI study of cognitive reappraisal in children, adolescents and young adults. Soc Cogn Affect Neurosci. 2012 1;7(1):11–22. [PubMed: 22228751]
38. Bremner JD, Vermetten E. Neuroanatomical Changes Associated with Pharmacotherapy in Posttraumatic Stress Disorder. Ann N Y Acad Sci. 2004 12 1;1032(1):154–7. [PubMed: 15677402]
39. Vermetten E, Vythilingam M, Southwick SM, Charney DS, Bremner JD. Long-term treatment with paroxetine increases verbal declarative memory and hippocampal volume in posttraumatic stress disorder. Biol Psychiatry. 2003 10 1;54(7):693–702. [PubMed: 14512209]
40. Yang Z, Oathes DJ, Linn KA, Bruce SE, Satterthwaite TD, Cook PA, et al. Cognitive Behavioral Therapy Is Associated With Enhanced Cognitive Control Network Activity in Major Depression and Posttraumatic Stress Disorder. Biol Psychiatry Cogn Neurosci Neuroimaging. 2018 4 1;3(4): 311–9. [PubMed: 29628063]
41. MacNamara A, Rabinak CA, Kennedy AE, Fitzgerald DA, Liberzon I, Stein MB, et al. Emotion Regulatory Brain Function and SSRI Treatment in PTSD: Neural Correlates and Predictors of Change. Neuropsychopharmacology. 2016 1;41(2):611–8. [PubMed: 26111649]
42. Fonzo GA, Goodkind MS, Oathes DJ, Zaiko YV, Harvey M, Peng KK, et al. Selective Effects of Psychotherapy on Frontopolar Cortical Function in PTSD. Am J Psychiatry. 2017 Jul 18;appi.ajp. 2017.16091073.
43. Teicher MH, Samson JA. Annual Research Review: Enduring neurobiological effects of childhood abuse and neglect. J Child Psychol Psychiatry. 2016 3;57(3):241–66. [PubMed: 26831814]

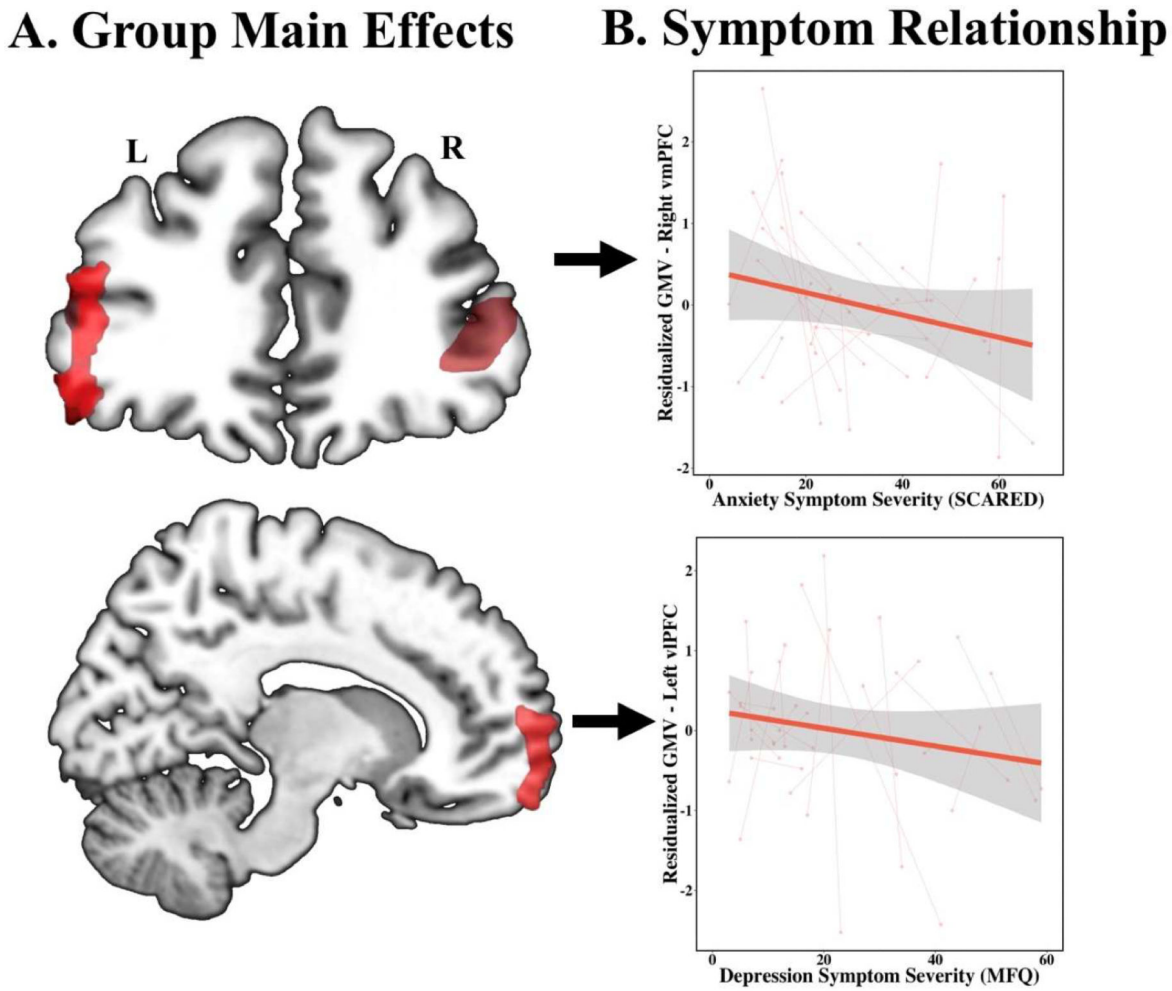

Figure 1: Gray matter abnormalities and symptom correlations in pediatric PTSD (n=22) as compared to TD youth (n=20).

(A) Reduced grey matter volume in the bilateral vlPFC and the right vmPFC in youth with PTSD as compared to TD youth (n=20), covaried for age at baseline, sex, total intracranial volume, and subject as a random effect. (B) Depression symptoms of PTSD, as measured by the MFQ, are inversely correlated with bilateral vlPFC gray matter volume and anxiety symptoms, as measured by the SCARED, are inversely correlated with vmPFC gray matter volume, covaried for age at baseline, sex, total intracranial volume, subject as a random effect, and the four alternative symptom scores (PTSD-RI cluster B, C, D, and SCARED). Scatterplot shows extracted cluster data in relation to depression symptom severity. *Abbreviations:* PTSD, post-traumatic stress disorder; TD, typically developing; vlPFC, ventrolateral prefrontal cortex; MFQ, Mood and Feelings Questionnaire; vmPFC, ventromedial prefrontal cortex; SCARED, Screen for Child Anxiety Related Disorders.

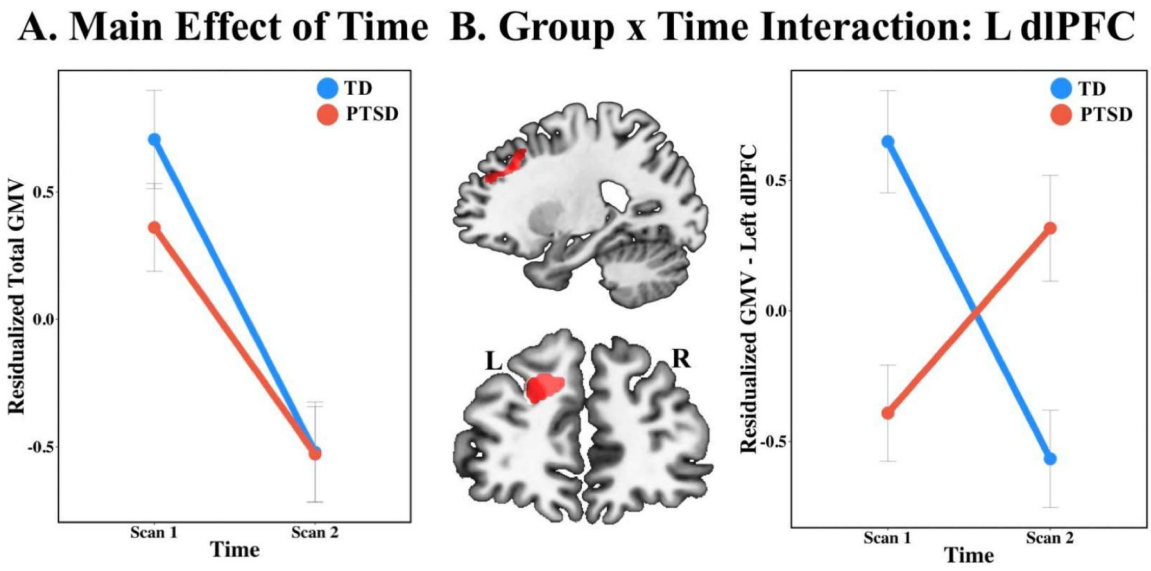

Figure 2: Longitudinal gray matter abnormalities and symptom correlations in pediatric PTSD (n=22) as compared to TD youth (n=20)

(A) Global decreases in gray matter volume with time for both TD youth and youth with PTSD as shown by a main effect of scan, covaried for age at baseline, sex, total intracranial volume, and subject as a random effect (k=133,285). (B) A group x time interaction, covaried for age at baseline, sex, total intracranial volume, and subject as a random effect, revealed that time positively predicted GMV in the left dlPFC in youth with PTSD, but negatively predicted GMV in TD youth (k=649; p=0.05).

Abbreviations: GMV, gray matter volume; PTSD, post-traumatic stress disorder; TD, typically developing; dlPFC, dorsolateral prefrontal cortex.

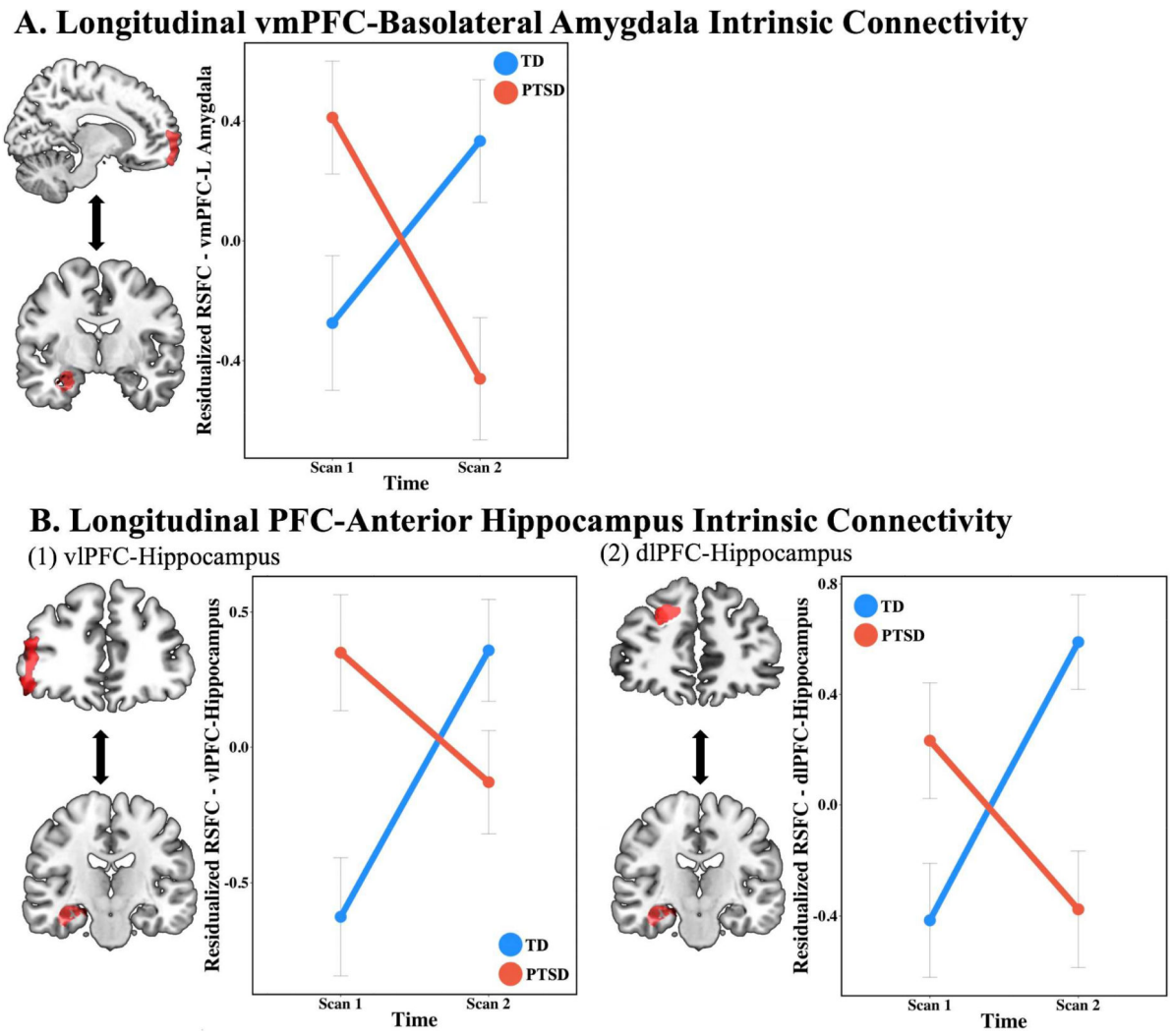

Figure 3: Longitudinal prefrontal intrinsic connectivity abnormalities and symptom correlations in pediatric PTSD (n=22) as compared to TD youth (n=20).

(A) Longitudinal changes in resting state connectivity using the right vmPFC cluster identified in the VBM analyses as a seed region. A significant group by time interaction, covaried for age at baseline, sex, and subject as a random effect, revealed that intrinsic connectivity between the vmPFC and right basolateral amygdala exhibited longitudinal increases in TD youth and longitudinal decreases in youth with PTSD. (B)(1) Longitudinal changes in resting state connectivity using the left vlPFC cluster identified in the VBM analyses as a seed region. A significant group by time interaction, covaried for age at baseline, sex, and subject as a random effect, revealed that intrinsic connectivity between the vlPFC and the anterior hippocampus exhibited longitudinal increases in TD youth and longitudinal decreases in youth with PTSD. (2) A similar trending group by time interaction with the anterior hippocampus was identified using the dlPFC cluster identified in VBM analyses as a seed region. For graphing and post-hoc analyses, the average connectivity estimate was extracted for significant clusters.

Abbreviations: vmPFC, ventromedial prefrontal cortex; PFC, prefrontal cortex; vlPFC, ventrolateral prefrontal cortex; dlPFC, dorsolateral prefrontal cortex; GMV, gray matter volume; PTSD, posttraumatic stress disorder; TD, typically developing.

Table 1 –

Full Sample Participant Characteristics.

The control and PTSD groups did not differ significantly in sex distribution, age, or Tanner stage. The healthy group had significantly higher IQ scores while the PTSD group had significantly higher MFQ and SCARED scores. The PTSD Reaction Index, MFQ, and SCARED represent the youth report scores. Numbers in parentheses represent the standard deviation.

	TD (n=22, F=17)		PTSD (n=27, F=18)		Group Comparison	
	Time 1	*Time 2*	*Time 1*	*Time 2*	*t*	*p*
Age (years)	13.92 (2.44)	15.17 (2.49)	14.01 (2.81)	15.51 (3.15)	0.35	0.73
Age range	10.34–17.99	11.47–19.31	8.07–17.99	9.17–23.4		
IQ (avg)	110	111.14	102.23	100.89	3.08	0.0028
Tanner	3.29	3.79	2.94	3.85	0.7	0.49
MFQ	3.05	3.95	24.56	20.29	−7.21	<0.0001
SCARED	9.2	8.5	34.67	26	−7.62	<0.0001

Abbreviations: MFQ, Mood and Feelings Questionnaire; SCARED, Screen for Child Anxiety Related Mood Disorders;

Table 2 –

Additional PTSD Characteristics

The CAPS-CA score was not obtained for the first five PTSD participants.

	PTSD (n=27, F=18)	
	Time 1	***Time 2***
CAPS-CA	72.38	49.34
PTSD-RI	49.67	35.67
Index Trauma (n)	Sexual Abuse (8), Physical Abuse/Neglect (0), Witnessing Violence (3), Traumatic Accident/Death (11)	
Comorbid diagnoses (n)	Generalized Anxiety Disorder (5), MDD single episode (10), MDD recurrent (2), ADHD-inattentive type (4), ADHD-hyperactive type (1), ADHD-combined type (3), Social Anxiety Disorder (4), Separation Anxiety Disorder (9), NOS (3), Depressive Disorder (2)	Generalized Anxiety Disorder (4), MDD single episode (5), MDD recurrent (0), ADHD-inattentive type (6), Social Anxiety Disorder (3), Separation Anxiety Disorder (2), NOS (1), Depressive Disorder (1), Polysubstance Dependence (2), Adjustment Disorder with depressed moods (1), Oppositional Defiant Disorder (1)
Psychiatric medication (n)	alpha-agonist (1), SSRI (3), stimulant (8), benzodiazepine (2), antipsychotic (1), anxiolytic (1), serotonin anatagonist (1), antihistamine (2)	alpha-agonist (4), SSRI (11), stimulant (8), benzodiazepine (1), serotonin anatagonist (4), antihistamine (4), NRI (1), serotonin-norepinephrine reuptake inhibitor (1), lithium (1), TCA (1), anticonvulsant/ antiepileptic (1), anxiolytic (1)

Abbreviations: CAPS-CA, Clinician-Administered PTSD Scale Child and Adolescent version; PTSD-RI, PTSD Reaction Index

Table 3 –
Summary of Structural MRI Longitudinal Analyses.

Clusters shown survived whole-brain cluster correction (corrected < 0.05). Peak coordinates (x, y, z) are reported based on the MNI atlas in LPI orientation. All analyses included age at baseline, sex, and total intracranial volume as covariates.

Whole-Brain Voxel-Based Morphometry (VBM)

Contrast	Region	Laterality	BA	Peak Z	x	y	z	Cluster Voxels
TD > PTSD	vlPFC	R	45/47	3.27	−43.5	−43.5	−3	1653
	PCC	B	31	3.39	−1.5	75.5	36	1082
	Precentral Gyrus	R	44	3.61	−60	−4.5	22.5	951
	vlPFC	L	45/47	3.38	45	−37.5	6	910
	vmPFC	R	10/11	3.57	−10.5	−64.5	−10.5	702
Group x Time *PTSD>TD*	dlPFC	L	9	2.83	22.5	−27	43.5	649

Abbreviations: vmPFC, ventromedial PFC; vlPFC, ventrolateral PFC; PCC, posterior cingulate cortex; vmPFC, ventromedial prefrontal cortex; dlPFC, dorsolateral prefrontal cortex.

Table 4 – Summary RSFC Longitudinal Analyses.

Clusters shown survived cluster correction (corrected < 0.05) within the limbic mask. Peak coordinates (x, y, z) are reported based on the MNI atlas in LPI orientation. All analyses included age at baseline, sex, and subject as a random effect. Italics indicates a trending effect following correction (p<0.08).

Seed-Based Resting-State Functional Connectivity (RSFC)									
Contrast	**Mask**	**Seed**	**Target**	**Laterality**	**Peak Z**	**k**	**x**	**y**	**z**
Group x Time	Limbic	R vmPFC	Amygdala	L	−3.79	26	26	8	−16
	Limbic	L vlPFC	Hippocampus	L	−3.95	22	32	12	−18
	Limbic	*L dlPFC*	*Hippocampus*	L	*−3.22*	*17*	*34*	*18*	*−24*
	Limbic	PCC	Amygdala	L	3.9	16	28	10	−16

Abbreviations: vmPFC, ventromedial PFC; vlPFC, ventrolateral prefrontal cortex; dlPFC, dorsolateral prefrontal cortex.